Research Article | Vol. 9, No. 4 | 1 Apr 2018 | BIOMEDICAL OPTICS EXPRESS 1916
Biomedical Optics EXPRESS

Decreased resting-state brain signal complexity in patients with mild cognitive impairment and Alzheimer's disease: a multi-scale entropy analysis

Xuanyu Li,[1,11] Zhaojun Zhu,[2,3,11] Weina Zhao,[1,4,11] Yu Sun,[1] Dong Wen,[5,6] Yunyan Xie,[1] Xiangyu Liu,[7] Haijing Niu,[2,3,12] and Ying Han[1,8,9,10,13]

[1]*Department of Neurology, XuanWu Hospital of Capital Medical University, Beijing, 100053, China*
[2]*State Key Laboratory of Cognitive Neuroscience and Learning & IDG/McGovern Institute for Brain Research, Beijing Normal University, Beijing, China*
[3]*Center for Collaboration and Innovation in Brain and Learning Sciences, Beijing Normal University, Beijing, 100875, China*
[4]*Department of Neurology, Mudanjiang Medical University Affiliated HongQi Hospital, Mudanjiang, 157000, China*
[5]*School of Information Science and Engineering, Yanshan University, 438 Hebei Avenue, Qinhuangdao, 066004, China*
[6]*The Key Laboratory of Software Engineering of Hebei Province, Yanshan University, 438 Hebei Avenue, Qinhuangdao, 066004, China*
[7]*Shenzhen Longhua District Central Hospital, Shenzhen, 518110, China*
[8]*Center of Alzheimer's Disease, Beijing Institute for Brain Disorders, Beijing, 100053, China*
[9]*Beijing Institute of Geriatrics, Beijing, 100053, China*
[10]*National Clinical Research Center for Geriatric Disorders, Beijing, 100053, China*
[11]*Xuanyu Li, Zhaojun Zhu, and Weina Zhao contributed equally to this research*
[12]*niuhjing@bnu.edu.cn*
[13]*hanying@xwh.ccmu.edu.cn*

Abstract: Multiscale entropy (MSE) analysis is a novel entropy-based analysis method for quantifying the complexity of dynamic neural signals and physiological systems across multiple temporal scales. This approach may assist in elucidating the pathophysiologic mechanisms of amnestic mild cognitive impairment (aMCI) and Alzheimer's disease (AD). Using resting-state fNIRS imaging, we recorded spontaneous brain activity from 31 healthy controls (HC), 27 patients with aMCI, and 24 patients with AD. The quantitative analysis of MSE revealed that reduced brain signal complexity in AD patients in several networks, namely, the default, frontoparietal, ventral and dorsal attention networks. For the default and ventral attention networks, the MSE values also showed significant positive correlations with cognitive performances. These findings demonstrated that the MSE-based analysis method could serve as a novel tool for fNIRS study in characterizing and understanding the complexity of abnormal cortical signals in AD cohorts.

OCIS codes: (170.2655) Functional monitoring and imaging; (170.5380) Physiology; (170.3880) Medical and biological imaging.

References and links

1. P. Scheltens, K. Blennow, M. M. Breteler, B. de Strooper, G. B. Frisoni, S. Salloway, and W. M. Van der Flier, "Alzheimer's disease," Lancet **388**(10043), 505–517 (2016).
2. K. M. Langa and D. A. Levine, "The diagnosis and management of mild cognitive impairment: a clinical review," JAMA **312**(23), 2551–2561 (2014).
3. R. C. Petersen, "Mild cognitive impairment as a diagnostic entity," J. Intern. Med. **256**(3), 183–194 (2004).
4. B. C. Dickerson and R. A. Sperling, "Large-scale functional brain network abnormalities in Alzheimer's disease: insights from functional neuroimaging," Behav. Neurol. **21**(1), 63–75 (2009).

#322912 https://doi.org/10.1364/BOE.9.001916
Journal © 2018 Received 9 Feb 2018; revised 20 Mar 2018; accepted 20 Mar 2018; published 26 Mar 2018

Biomedical Optics EXPRESS

5. H. J. Li, X. H. Hou, H. H. Liu, C. L. Yue, Y. He, and X. N. Zuo, "Toward systems neuroscience in mild cognitive impairment and Alzheimer's disease: a meta-analysis of 75 fMRI studies," Hum. Brain Mapp. **36**(3), 1217–1232 (2015).
6. I. M. McDonough and K. Nashiro, "Network complexity as a measure of information processing across resting-state networks: evidence from the Human Connectome Project," Front. Hum. Neurosci. **8**, 409 (2014).
7. M. Costa, A. L. Goldberger, and C. K. Peng, "Multiscale entropy analysis of complex physiologic time series," Phys. Rev. Lett. **89**(6), 068102 (2002).
8. B. Manor and L. A. Lipsitz, "Physiologic complexity and aging: implications for physical function and rehabilitation," Prog. Neuropsychopharmacol. Biol. Psychiatry **45**, 287–293 (2013).
9. M. Costa, A. L. Goldberger, and C. K. Peng, "Multiscale entropy analysis of biological signals," Phys. Rev. E Stat. Nonlin. Soft Matter Phys. **71**(2 Pt 1), 021906 (2005).
10. D. R. Chialvo, "Physiology: unhealthy surprises," Nature **419**(6904), 263 (2002).
11. A. C. Yang, S. J. Wang, K. L. Lai, C. F. Tsai, C. H. Yang, J. P. Hwang, M. T. Lo, N. E. Huang, C. K. Peng, and J. L. Fuh, "Cognitive and neuropsychiatric correlates of EEG dynamic complexity in patients with Alzheimer's disease," Prog. Neuropsychopharmacol. Biol. Psychiatry **47**, 52–61 (2013).
12. T. Mizuno, T. Takahashi, R. Y. Cho, M. Kikuchi, T. Murata, K. Takahashi, and Y. Wada, "Assessment of EEG dynamical complexity in Alzheimer's disease using multiscale entropy," Clin. Neurophysiol. **121**(9), 1438–1446 (2010).
13. J. Escudero, D. Abásolo, R. Hornero, P. Espino, and M. López, "Analysis of electroencephalograms in Alzheimer's disease patients with multiscale entropy," Physiol. Meas. **27**(11), 1091–1106 (2006).
14. P. H. Tsai, S. C. Chang, F. C. Liu, J. Tsao, Y. H. Wang, and M. T. Lo, "A Novel Application of Multiscale Entropy in Electroencephalography to Predict the Efficacy of Acetylcholinesterase Inhibitor in Alzheimer's Disease," Comput. Math. Methods Med. **2015**, 953868 (2015).
15. C. Y. Liu, A. P. Krishnan, L. Yan, R. X. Smith, E. Kilroy, J. R. Alger, J. M. Ringman, and D. J. Wang, "Complexity and synchronicity of resting state blood oxygenation level-dependent (BOLD) functional MRI in normal aging and cognitive decline," J. Magn. Reson. Imaging **38**(1), 36–45 (2013).
16. M. A. Kamran, M. M. Mannan, and M. Y. Jeong, "Cortical Signal Analysis and Advances in Functional Near-Infrared Spectroscopy Signal: A Review," Front. Hum. Neurosci. **10**, 261 (2016).
17. G. McKhann, D. Drachman, M. Folstein, R. Katzman, D. Price, and E. M. Stadlan, "Clinical diagnosis of Alzheimer's disease: report of the NINCDS-ADRDA Work Group* under the auspices of Department of Health and Human Services Task Force on Alzheimer's Disease," Neurology **34**(7), 939–944 (1984).
18. Z. Li, H. Liu, X. Liao, J. Xu, W. Liu, F. Tian, Y. He, and H. Niu, "Dynamic functional connectivity revealed by resting-state functional near-infrared spectroscopy," Biomed. Opt. Express **6**(7), 2337–2352 (2015).
19. H. Niu and Y. He, "Resting-state functional brain connectivity: lessons from functional near-infrared spectroscopy," The Neuroscientist : a review journal bringing neurobiology, neurology and psychiatry **20**(2), 173–188 (2014).
20. H. Niu, Z. Li, X. Liao, J. Wang, T. Zhao, N. Shu, X. Zhao, and Y. He, "Test-retest reliability of graph metrics in functional brain networks: a resting-state fNIRS study," PLoS One **8**(9), e72425 (2013).
21. B. T. Yeo, F. M. Krienen, J. Sepulcre, M. R. Sabuncu, D. Lashkari, M. Hollinshead, J. L. Roffman, J. W. Smoller, L. Zöllei, J. R. Polimeni, B. Fischl, H. Liu, and R. L. Buckner, "The organization of the human cerebral cortex estimated by intrinsic functional connectivity," J. Neurophysiol. **106**(3), 1125–1165 (2011).
22. H. Zhang, Y. J. Zhang, C. M. Lu, S. Y. Ma, Y. F. Zang, and C. Z. Zhu, "Functional connectivity as revealed by independent component analysis of resting-state fNIRS measurements," Neuroimage **51**(3), 1150–1161 (2010).
23. S. Kohno, I. Miyai, A. Seiyama, I. Oda, A. Ishikawa, S. Tsuneishi, T. Amita, and K. Shimizu, "Removal of the skin blood flow artifact in functional near-infrared spectroscopic imaging data through independent component analysis," J. Biomed. Opt. **12**(6), 062111 (2007).
24. B. R. White, A. Z. Snyder, A. L. Cohen, S. E. Petersen, M. E. Raichle, B. L. Schlaggar, and J. P. Culver, "Resting-state functional connectivity in the human brain revealed with diffuse optical tomography," Neuroimage **47**(1), 148–156 (2009).
25. B. Biswal, F. Z. Yetkin, V. M. Haughton, and J. S. Hyde, "Functional connectivity in the motor cortex of resting human brain using echo-planar MRI," Magn. Reson. Med. **34**(4), 537–541 (1995).
26. J. Xu, X. Liu, J. Zhang, Z. Li, X. Wang, F. Fang, and H. Niu, "FC-NIRS: a functional connectivity analysis tool for near-infrared spectroscopy data," BioMed Res. Int. **2015**, 248724 (2015).
27. X. Cui, D. M. Bryant, and A. L. Reiss, "NIRS-based hyperscanning reveals increased interpersonal coherence in superior frontal cortex during cooperation," Neuroimage **59**(3), 2430–2437 (2012).
28. A. C. Yang, S. J. Tsai, C. H. Yang, C. H. Kuo, T. J. Chen, and C. J. Hong, "Reduced physiologic complexity is associated with poor sleep in patients with major depression and primary insomnia," J. Affect. Disord. **131**(1-3), 179–185 (2011).
29. T. Takahashi, R. Y. Cho, T. Mizuno, M. Kikuchi, T. Murata, K. Takahashi, and Y. Wada, "Antipsychotics reverse abnormal EEG complexity in drug-naive schizophrenia: a multiscale entropy analysis," Neuroimage **51**(1), 173–182 (2010).
30. P. R. Norris, J. A. Canter, J. M. Jenkins, J. H. Moore, A. E. Williams, and J. A. Morris, Jr., "Personalized medicine: genetic variation and loss of physiologic complexity are associated with mortality in 644 trauma patients," Ann. Surg. **250**(4), 524–530 (2009).

Biomedical Optics EXPRESS

31. D. Cheng, S. J. Tsai, C. J. Hong, and A. C. Yang, "Reduced physiological complexity in robust elderly adults with the APOE epsilon4 allele," PLoS One **4**(11), e7733 (2009).
32. A. C. Yang, C. C. Huang, H. L. Yeh, M. E. Liu, C. J. Hong, P. C. Tu, J. F. Chen, N. E. Huang, C. K. Peng, C. P. Lin, and S. J. Tsai, "Complexity of spontaneous BOLD activity in default mode network is correlated with cognitive function in normal male elderly: a multiscale entropy analysis," Neurobiol. Aging **34**(2), 428–438 (2013).
33. G. Tononi, G. M. Edelman, and O. Sporns, "Complexity and coherency: integrating information in the brain," Trends Cogn. Sci. (Regul. Ed.) **2**(12), 474–484 (1998).
34. J. Jeong, "EEG dynamics in patients with Alzheimer's disease," Clin. Neurophysiol. **115**(7), 1490–1505 (2004).
35. B. Jelles, J. H. van Birgelen, J. P. Slaets, R. E. Hekster, E. J. Jonkman, and C. J. Stam, "Decrease of non-linear structure in the EEG of Alzheimer patients compared to healthy controls," Clin. Neurophysiol. **110**(7), 1159–1167 (1999).
36. G. Tononi, O. Sporns, and G. M. Edelman, "A measure for brain complexity: relating functional segregation and integration in the nervous system," Proc. Natl. Acad. Sci. U.S.A. **91**(11), 5033–5037 (1994).
37. K. J. Friston, G. Tononi, O. Sporns, and G. Edelman, "Characterising the complexity of neuronal interactions," Hum. Brain Mapp. **3**(4), 302–314 (1995).
38. X. Delbeuck, M. Van der Linden, and F. Collette, "Alzheimer's disease as a disconnection syndrome?" Neuropsychol. Rev. **13**(2), 79–92 (2003).
39. D. Kapogiannis and M. P. Mattson, "Disrupted energy metabolism and neuronal circuit dysfunction in cognitive impairment and Alzheimer's disease," Lancet Neurol. **10**(2), 187–198 (2011).
40. R. L. Buckner, A. Z. Snyder, B. J. Shannon, G. LaRossa, R. Sachs, A. F. Fotenos, Y. I. Sheline, W. E. Klunk, C. A. Mathis, J. C. Morris, and M. A. Mintun, "Molecular, structural, and functional characterization of Alzheimer's disease: evidence for a relationship between default activity, amyloid, and memory," The Journal. of neurosci : the official journal of the Society for Neuroscience **25**(34), 7709–7717 (2005).
41. T. P. Zanto and A. Gazzaley, "Fronto-parietal network: flexible hub of cognitive control," Trends Cogn. Sci. (Regul. Ed.) **17**(12), 602–603 (2013).
42. M. W. Cole, J. R. Reynolds, J. D. Power, G. Repovs, A. Anticevic, and T. S. Braver, "Multi-task connectivity reveals flexible hubs for adaptive task control," Nat. Neurosci. **16**(9), 1348–1355 (2013).
43. Z. Zhang, H. Zheng, K. Liang, H. Wang, S. Kong, J. Hu, F. Wu, and G. Sun, "Functional degeneration in dorsal and ventral attention systems in amnestic mild cognitive impairment and Alzheimer's disease: an fMRI study," Neurosci. Lett. **585**, 160–165 (2015).
44. R. Li, X. Wu, A. S. Fleisher, E. M. Reiman, K. Chen, and L. Yao, "Attention-related networks in Alzheimer's disease: a resting functional MRI study," Hum. Brain Mapp. **33**(5), 1076–1088 (2012).
45. H. Li, J. Jia, and Z. Yang, "Mini-Mental State Examination in Elderly Chinese: A Population-Based Normative Study," J. Alzheimers Dis. **53**(2), 487–496 (2016).
46. J. Lu, D. Li, F. Li, A. Zhou, F. Wang, X. Zuo, X. F. Jia, H. Song, and J. Jia, "Montreal cognitive assessment in detecting cognitive impairment in Chinese elderly individuals: a population-based study," J. Geriatr. Psychiatry Neurol. **24**(4), 184–190 (2011).
47. M. D. Greicius, G. Srivastava, A. L. Reiss, and V. Menon, "Default-mode network activity distinguishes Alzheimer's disease from healthy aging: evidence from functional MRI," Proc. Natl. Acad. Sci. U.S.A. **101**(13), 4637–4642 (2004).
48. M. D. Greicius, B. Krasnow, A. L. Reiss, and V. Menon, "Functional connectivity in the resting brain: a network analysis of the default mode hypothesis," Proc. Natl. Acad. Sci. U.S.A. **100**(1), 253–258 (2003).
49. M. Corbetta and G. L. Shulman, "Control of goal-directed and stimulus-driven attention in the brain," Nat. Rev. Neurosci. **3**(3), 201–215 (2002).

1. Introduction

Alzheimer's disease (AD) is the most common progressive neurodegenerative disease and one of the greatest healthcare challenges of the 21st century [1]. Amnestic mild cognitive impairment (aMCI), regarded as a prodromal stage of AD, is characterized by early memory decline without evidence of a significant impairment in daily activities [2, 3]. In recent decades, concepts from non-medical disciplines, such as mathematics, physics and computer science, have been increasingly employed in the imaging study of AD to better understand the complex pathological mechanisms of the disease.

Network science, combined with non-invasive functional imaging, has generated unprecedented insights regarding the adult brain's functional organization and promises to help elucidate the development of the functional architectures that support complex behavior. In this context, AD is increasingly viewed as a disease with multiple dysfunctional large-scale neuronal networks rather than a localized abnormality [4]. A meta-analysis of 75 fMRI studies [5] suggested that MCI and AD showed different hypoactivation patterns, whereas similar compensatory large-scale networks are used to fulfill cognitive tasks. This large-scale

Biomedical Optics EXPRESS

network approach may help evaluating the physiopathological progression of AD at a system level.

Using fundamental nonlinear theory, the activity of neural networks can be described as nonlinear dynamic processes that are regulated by couplings and feedback loops within and across multiple temporal and spatial scales. However, by concentrating efforts on understanding spatial disorganization across cortical regions, this research has largely ignored the temporal disorganization of neural dynamics in AD patients. Accumulating evidence suggests that complexity analysis, a nonlinear estimation approach of dynamical brain activity, conveys important information regarding network dynamics [6] and can thus be of great value for investigating temporal disorganization in AD.

Complexity analysis is most often performed using entropy-based algorithms by quantifying the regularity and predictability of a time series [7]. The complexity of a physiological system may be fundamentally associated with its ability to adapt to a changing environment [8]. Thus, the loss of complexity has been suggested as the hallmark of aging and various clinical conditions. As discussed in depth by Costa et al [7, 9], complexity is associated with "meaningful structural richness"; both completely regular and completely random signals are not truly complex. Notably, traditional entropy-based approaches estimate the degree of regularity of a time series on a single time scale. Entropy increases with the degree of irregularity, peaking in completely random systems. When applied to a physiologic time series, the conventional entropy-based approach can yield contradictory results, e.g., a high degree of entropy in pathological conditions, such as heart rate rhythm in atrial fibrillation [7, 9].

To overcome this issue, multiscale entropy (MSE) analysis has been developed and shown to effectively quantify the dynamic complexity in physiological systems [7, 9]. In contrast to the traditional entropy approach, the MSE approach makes use of a method termed "coarse-graining," which provides a profile of entropy across multiple time scales; in this way, meaningful complexity and uncorrelated randomness can be differentiated [7, 10]. Prior studies have demonstrated the utility of MSE in exploring changes in electroencephalography (EEG) signals from AD patients [11–13]. These previous analysis have generally shown that AD patients have reduced MSE values compared with healthy controls, which is consistent with findings from nonlinear EEG analysis in this population. Furthermore, MSE analysis of EEG signals may have the potential to predict the efficacy of acetylcholinesterase inhibitors prior to therapy [14]. However, our understanding of the temporal properties of abnormal hemoglobin signals from aMCI and AD patients is fairly limited. Although it has been suggested that cognitive impairment is related to reduced regional approximate entropy in subjects with familial AD [15], improvements in complexity analyses, such as MSE, are required. Moreover, the long sampling rate and short time series of fMRI permit few reliable time scales to be included in the analysis. For these reasons, the estimation of MSE can be biased for large-scale factors.

Functional near-infrared spectroscopy (fNIRS) is a noninvasive neuroimaging technique used to simultaneously measure the concentration changes of cerebral oxyhemoglobin and deoxyhemoglobin [16]. The signal from this technique has a similar physiological basis with the resting-state BOLD signal from functional MRI. Due to its high sampling rate, fNIRS was used in the present study to provide rich temporal information for investigating the complex dynamics of brain hemoglobin signals. Here, we aimed to investigate brain signal complexity in aMCI and AD patients using MSE. To this end, we conducted a resting fNIRS experiment on a cohort of aMCI and AD patients and healthy controls. We hypothesized that the patient groups would show decreased brain signal complexity compared with healthy controls and that such complexity disturbances would correlate with cognitive dysfunction.

Biomedical Optics EXPRESS

2. Materials and methods

2.1 Participants

Eighty-seven right-handed participants were recruited for this study, comprising 27 AD patients (12 men and 15 women), 29 aMCI patients (14 men and 15 women) and 31 sex-, age-, and education-matched healthy controls (HC: 11 men and 20 women). For each participant, written informed consent was obtained before the beginning of the experiment. Patients with aMCI and AD were recruited from patients complaining of memory loss who had visited a memory clinic at the Neurology Department in XuanWu Hospital of Capital Medical University, Beijing, China. The healthy controls were enrolled from the local community by advertisements. This study was approved by the Medical Research Ethics Committee of XuanWu Hospital. The diagnosis of AD was determined by the published diagnostic criteria (Association, 1994; Dubios B et al., 2007 [17]: (1) meeting the criteria for dementia; (2) gradual and progressive change in memory function over more than 6 months; (3) impaired episodic memory on objective testing; (4) hippocampal atrophy confirmed by structural MRI. The inclusion criteria for aMCI were defined as: (1) memory complaint, preferably confirmed by someone familiar with the patient; (2) objective memory impairment; (3) normal or near-normal performance on global cognitive tests after age-, gender-, and education-adjusted; (4) a total Clinical Dementia Rating (CDR) score ≤ 0.5; and (5) absence of dementia. The inclusion criteria for HC were as follows: (1) having no report of any cognition complaint; (2) normal performance on global cognitive tests, adjusted for age, gender and education; (3) the CDR score of 0. The exclusion criteria for all of the participants were as follows: (1) having suffered from stroke; (2) having a Hamilton Depression Rating Scale score greater than 24 points; (3) having other nervous system or systemic diseases, which can cause cognitive impairment; (4) having a history of psychosis or congenital mental growth retardation; (5) having contraindications for MRI. We assessed all of the participants using a standardized clinical evaluation protocol that comprised the Mini-Mental State Examination (MMSE), the Montreal Cognitive Assessment (MoCA), and the Auditory Verbal Learning Test (AVLT). Detailed demographics and clinical characteristics of the participants are shown in Table 1.

Table 1. Demographics and clinical characters of the participants

Characteristics	HC	aMCI	AD	*p*-value
N (M/F)	31(11/20)	27(14/13)	24(9/15)	0.40[a]
Age (years)	67.61±8.86	70.33±8.27	72.25±9.15	0.15[b]
Education (years)	11.77±6.25	10.74±4.97	9.67±4.60	0.30[b]
MMSE	28.26±3.02	23.69±4.71	15.54±5.62	<0.01[b]
MOCA	25.61±3.77	19.22±5.15	10.67±5.11	<0.01[b]
AVLT_I	9.82±2.27	6.28±2.64	3.57±2.01	<0.01[b]
AVLT_D	11.61±2.36	4.36±3.88	1.48±2.00	<0.01[b]
AVLT_R	13.10±1.70	8.08±3.58	4.26±2.94	<0.01[b]

The data are presented as the mean ± SD.

Abbreviations: aMCI, amnestic mild cognitive impairment; AD, Alzheimer's disease; MMSE, Mini-Mental State Examination; MOCA, Montreal Cognitive Assessment; AVLT, Auditory Verbal Learning Test (AVLT_I, AVLT_Immediate Recall; AVLT_D, AVLT_Delayed Recall; AVLT_R, AVLT_Recognition).

[a] The *p* value was calculated using a two-tail Pearson's chi-square test.

[b] The *p* value was calculated using one-way analysis of variance test.

2.2 fNIRS data acquisition

We used a continuous-wave near-infrared optical imaging system (CW6, TechEn Inc., MA, USA) to record hemoglobin oxygenation activity in the cerebral cortex of the participants. The data collection was performed in a dimly lit room in XuanWu Hospital. Similar to our

Biomedical Optics EXPRESS

previous study [18–20], the arrangement of the probe holder consisted of 12 light sources (each with two wavelengths: 670 and 830 nm) and 24 detectors that allowed for the frontal, temporal, parietal, and occipital lobes to be measured bilaterally (Fig. 1(B)). The distance between adjacent sources and detectors was set to 3.2 cm, resulting in 46 measurement channels for the entire cortex. During fNIRS scanning, the participants were instructed to keep relaxed with their eyes closed, without falling asleep, and to not think about anything in particular. The scanning duration was approximately 11 minutes for each participant. Of note, the positioning of the probe array was determined according to the international 10–20 system of electrode placement and used the external auditory canals and vertex of each participant as landmarks. The position of the probes relative to the landmarks was established to be repeatable across subjects. A structural MRI image of an arbitrarily selected participant was acquired and normalized to MNI space to validate the position of the channels; during the scan, the participant wore the probe holder with the sources and detectors replaced by vitamin E capsules. The measurement channels were projected on a functional network template from Yeo et al. [21], as shown in Fig. 1(C).

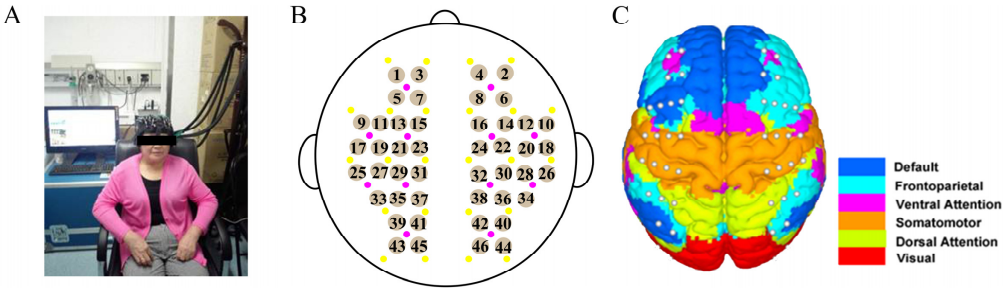

Fig. 1. Schematic diagram of experimental data acquisition. (A) Photo obtained during data collection. (B) The arrangement of the whole-head 46 measurement channels on a plane graph. (C) The arrangement of the whole-head 46 measurement channels on a functional network brain template [21].

2.3 Data preprocessing

The optical signal was first transformed into a time series of oxyhemoglobin (HbO) and deoxyhemoglobin (HbR) concentrations using the modified Beer-Lambert law. We then conducted a temporal ICA analysis using a publicly available software, *FastICA v2.5* (*www.cis.hut.fi/projects/ica/fastica/*) to remove typical motion-induced artifacts and systematic physiological noise [20, 22, 23]. The data were subsequently digitally bandpass filtered (0.009-0.08 Hz) to reduce the effects of low-frequency drift and high-frequency neurophysiological noise, as well as to obtain the low-frequency hemodynamic signals that are believed to characterize spontaneous neural activity [24, 25]. We lastly removed global signals using global signal regression and extracted 10-min data from the continuous time course of each participant to conduct brain signal complexity analysis. The data preprocessing was primarily conducted using an in-house *FC-NIRS* package (*http://www.nitrc.org/projects/fcnirs* [26]), which was developed using MATLAB 2010b (*www.mathworks.org*) in a 64-bit Windows 7 environment. During the data processing, the data from five of the subjects were excluded due to large head motion or poor optical contact between the probe and scalp (3 for AD and 2 for aMCI), and finally we used eight-two participants for the following data analysis. Considering that the HbO signal has a better signal-to-noise ratio than the HbR signal in fNIRS measurements [27], we primarily focused on the HbO signal for data analysis of brain signal complexity for all participant groups.

Biomedical Optics EXPRESS

2.4 Data analysis

2.4.1 Estimation of brain signal complexity

We adopted multiscale entropy (MSE) to estimate brain signal complexity [7, 9]. The MSE method can quantify the signal complexity of a time series by calculating the sample entropy over multiple timescales [7, 9]. The MSE algorithm is available at http://www.psynetresearch.org/tools.html, and the procedures involved in MSE calculation can be summarized in the following two steps [7, 9]: First, a "coarse-grained" process was applied to the original fNIRS time series $\{x_1,\ldots,x_i,\ldots,x_N\}$ to obtain downsampled time series. For example, for different timescales t (i.e., 1-30 for this study), the coarse-grained time series y^t were separately constructed by averaging data points within non-overlapping windows of length t. Each value of the coarse-grained time series, j, was calculated by:

$$y_j^t = \frac{1}{t}\sum_{i=(j-1)t+1}^{jt} x_i, \quad 1 \le j \le \frac{N}{t}. \tag{1}$$

Second, for each coarse-grained time series (i.e., the downsample time series), sample entropy was computed by applying to the following equation:

$$S_E(m,r) = \ln\frac{C_{m+1}(r)}{C_m(r)}, \tag{2}$$

where the pattern length, m, was set to 2, and it indicated two consecutive data points were used for pattern matching. The similarity criterion, r, was set to 0.2, and it indicated data points were considered to have indistinguishable amplitude values (i.e., to "match") if the absolute amplitude difference between them was ≤ 20% of the time series standard. The $C_m(r)$ was defined as:

$$C_m(r) = \frac{\text{number of pairs}(i,j) \text{ with } |v_i^m - v_j^m| < r \times STD(y)}{\text{number of all probable pairs}}. \tag{3}$$

$|v_i^m - v_j^m|$ denotes the Chebychev distance between two vectors, i.e., v_i^m and v_j^m. The vector v_i^m is defined as $v_i^m = \{y_i, y_{i+1}, \ldots, y_{i+m-1}\}$ and the vector v_j^m is defined as $v_i^m = \{y_j, y_{j+1}, \ldots, y_{j+m-1}\}$. As such, sample entropy across different temporal scales, i.e., the MSE, quantifies the signal variability by estimating the predictability of amplitude patterns across a time series of length N. Lower MSE values for the time series reflect lower degrees of indeterminacy or higher degrees of determinacy. In contrast, higher MSE values indicate more complex or richer information in the signal. As such, sample entropy across different temporal scales, i.e., the MSE, quantifies the signal variability by estimating the predictability of amplitude patterns across a time series of length N. Lower MSE values for the time series reflect lower degrees of indeterminacy or higher degrees of determinacy. In contrast, higher MSE values indicate more complex or richer information in the signal. In this study, the time series used to calculate MSE included 30000 time points, which mainly included low-frequency brain activity signal representing changes on the scale of ten to one-hundred seconds. Such data generally required much larger temporal scale for coarse graining to obtain multiple fractal property of the signal. Meantime, considering the large scale calculation need longer resting-state data acquisition and the reliability guidance of the sample entropy estimations, we calculated the MSE on a scale of 1 to 30 for each subject in the current study (with parameters $m = 2$ and $r = 0.2$) [28]. For individual resting fNIRS data, the MSE of the hemodynamic signal was computed through all measurement channels to create a whole-brain MSE parametric map for subsequent group analysis.

Biomedical Optics EXPRESS

2.4.2 Group differences in brain signal complexity

To examine group differences in brain signal complexity on a whole-brain scale, we calculated the whole-brain-averaged MSE values for each group. Also, to test our hypothesis that the difference in brain signal complexity among groups is dependent on different functional brain systems, we further categorized the whole brain system into 6 different functional brain networks (default, frontoparietal control, ventral attention, somatomotor, dorsal attention and visual networks), following Yeo et al.'s work [21]. For each brain network, we conducted separate statistical comparisons of brain signal complexity. The averaged MSE within each functional network was used as an index to represent information related to brain signal complexity in the same network.

2.4.3 Statistical analysis

For group effects in brain signal complexity within each functional network, comparisons were performed among the three groups (AD, aMCI and HC) using one-way analysis of variance (ANOVA) with post hoc 2-sample *t*-tests when needed ($p < 0.05$ after correcting for multiple comparisons). Parametric ANOVA was used, and $p < 0.05$ with Bonferroni correction was considered significant. The effects of age, gender, and years of education were removed for all of these analyses. Furthermore, to determine the statistical reliability of the above findings, bootstrap analysis of confidence intervals was conducted using 1,000 bootstrap samples. For each functional network, confidence intervals (95%) for the average brain signal complexity within each group were calculated based on the bootstrap. Differences in brain signal complexity between groups were determined via a lack of overlap in these confidence intervals.

2.4.4 Relationships between brain signal complexity and clinical variables

To test the association between brain signal complexity and clinical variables, correlation analyses were performed between MSE and clinical variables (MMSE, MoCA, AVLT-immediate recall, AVLT-delayed recall, and AVLT-recognition) in the combined AD and aMCI groups on each functional brain network, with a significance threshold of $p < 0.05$. Before these correlation analyses, the effects of age, gender, and years of education were removed by multiple linear regression. The reliability of the correlation was determined by bootstrapping-estimated 95% confidence intervals (1000 bootstrap samples).

3. Results

3.1 Demographic and clinical characteristics

The demographic data are shown in Table 1; there were no significant differences in age, gender, or years of education among the three groups of participants. However, the patient groups (aMCI and AD) had significantly lower scores on the MMSE ($p < 0.01$), MOCA ($p < 0.01$), AVLT-immediate recall ($p < 0.01$), AVLT delayed recall ($p < 0.01$), and AVLT-recognition ($p < 0.01$) relative to the HC group.

3.2 Integrated brain signal complexity

MSE was utilized to estimate brain signal complexity in both healthy controls and patients. For each participant, the sample entropy on each measurement channel was separately calculated from scale 1 to 30. Figure 2(A) shows an example of the spatial distribution of sample entropy across multiple temporal scales in a representative brain region (No. 37) and a representative subject (No. 10). For each profile curve, sample entropy shows a monotonic increase with the temporal scale, with smaller values at the fine scale and larger values at the coarse scale for all participants. Since different temporal scales can characterize both short and long range temporal dynamics, the increasing entropy demonstrated increasing signal complexity for brain time series from short to long-range temporal correlations. There was no

Biomedical Optics EXPRESS

interaction between the sample entropy curves for these participants. Similar profile curves were obtained for the grouped participants (Fig. 2(A)). These results were also observed in other brain regions. Thus, to provide a scale-independent index for the evaluation of brain signal complexity, we calculated the area under the curve (AUC, i.e., the integral) according to the MSE values. It has been established that such an averaging approach has the advantage of combining information from all scale factors [28]. Moreover, this approach is also similar to those used by previous MSE studies that analyzed other types of physiological signals [12, 29–32].

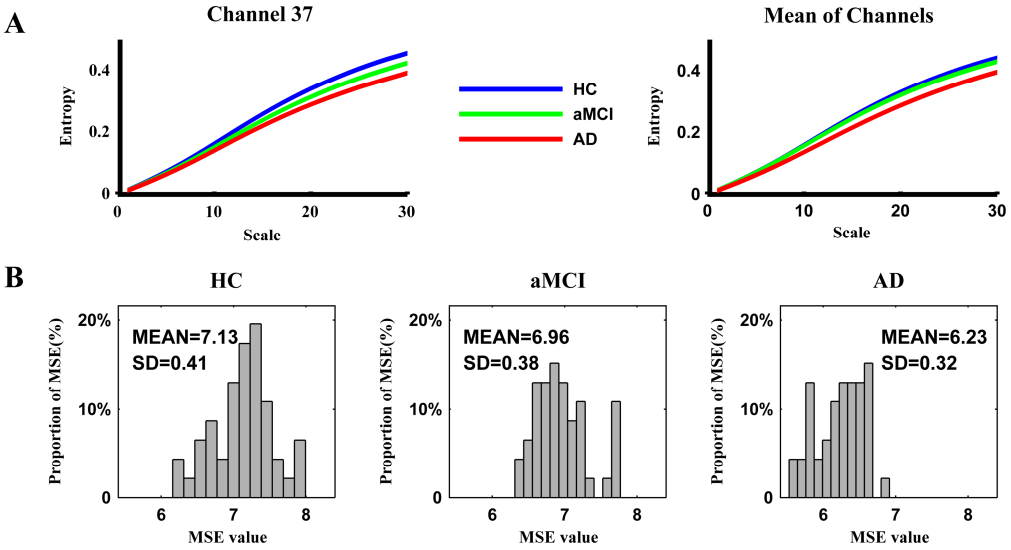

Fig. 2. The MSE and the distribution of MSE. (A) Sample entropy for participants in the HC, aMCI and AD groups, estimated for a specific brain region (i.e., channel No 37) and the whole brain, at different temporal scales. (B) The MSE distribution histogram of three groups of participants.

3.3 Group differences in brain signal complexity

The averaged MSE values across all 46 nodes were 7.13 ± 0.41 for HC, 6.96 ± 0.38 for aMCI, and 6.23 ± 0.32 for AD (Fig. 2(B)). Notably, the brain signal complexity in the HC group showed larger values in most brain regions compared to both aMCI and AD participants. A similar result was also found in the spatial maps of the MSE distribution in the three groups (Fig. 3(A)). The whole-brain-averaged MSE values also revealed significantly reduced brain signal complexity in the AD group (Fig. 3(B)).

Biomedical Optics EXPRESS

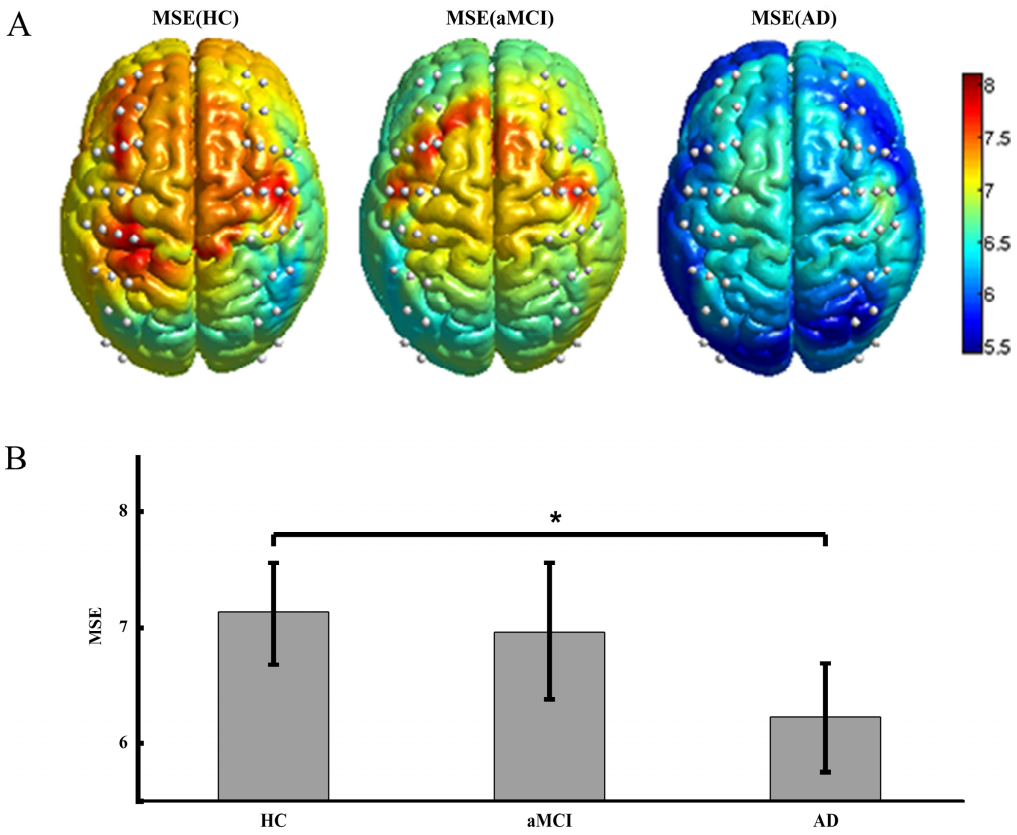

Fig. 3. Group difference analysis. (A) The spatial maps of MSE in HC, aMCI and AD groups, respectively. Interpolation algorithm was adopted to obtain smooth spatial maps. (B) Group differences in MSE values among HC, aMCI and AD groups. One asterisk represents significant group differences with a two sample *t*-test at $p < 0.05$ (Bonferroni corrected). The error bars indicate standard deviations.

For different functional brain networks, one-way ANOVA revealed network-associated differences in MSE among the three groups. The significant group differences in MSE were observed in the default mode ($F_{(2,\ 76)} = 3.88$, $p = 0.025$), frontoparietal ($F_{(2,\ 76)} = 2.59$, $p = 0.082$), and both dorsal ($F_{(2,\ 76)} = 2.58$, $p = 0.083$) and ventral attention networks ($F_{(2,\ 76)} = 3.66$, $p = 0.030$). However, no significant differences were found in the somatomotor or visual networks.

The MSE differences between the aMCI, AD and HC groups are shown in Fig. 4. Compared with HC, AD patients showed significant and reliable MSE decreases in the default mode ($t = 2.87$, $p = 0.018$, *Cohen's d* = 1.0), frontoparietal ($t = 2.19$, $p = 0.099$, *Cohen's d* = 0.81), dorsal ($t = 2.28$, $p = 0.084$, *Cohen's d* = 0.77) and ventral attention networks($t = 3.26$, $p = 0.006$, *Cohen's d* = 0.94). Likewise, compared to the aMCI patients, the AD patients also showed nearly significant and reliable decreases in MSE in the default mode network ($t = 2.29$, $p = 0.084$, *Cohen's d* = 0.81). Meantime, no MSE difference was observed for any brain network between the HC and aMCI groups.

Biomedical Optics EXPRESS

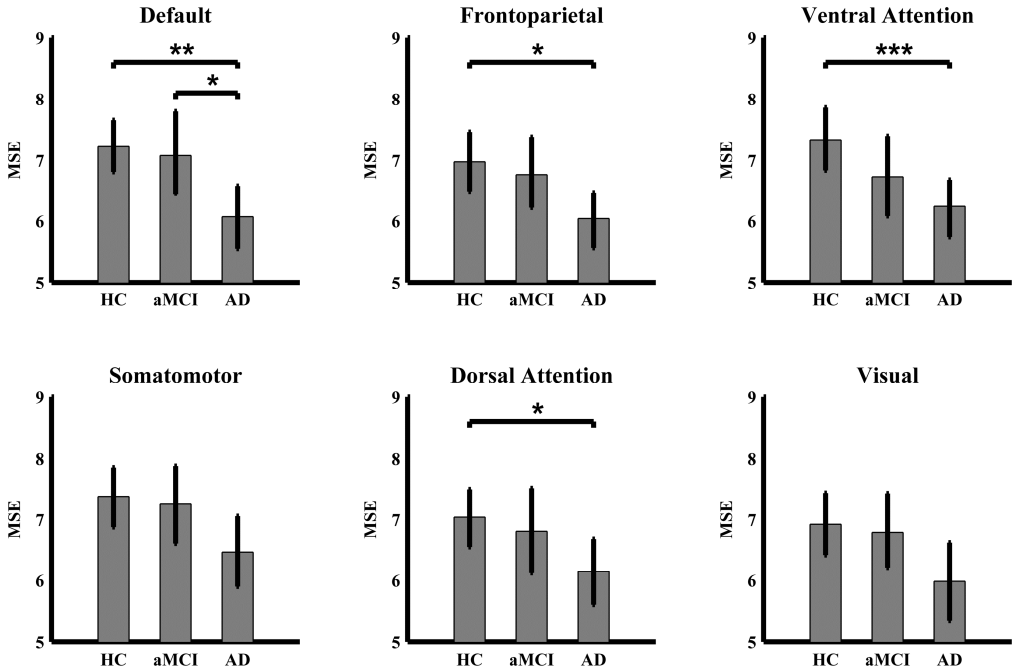

Fig. 4. Group differences in MSE values among HC, aMCI and AD in 6 functional networks. One, two and three asterisks represent significant group differences with a two sample *t*-test at $p < 0.1$, 0.05 and 0.01 (Bonferroni corrected). The error bars indicate standard deviations.

3.4 Relationships between brain signal complexity and clinical variables

When considering the patients with AD and aMCI, the brain signal complexity in the default mode network was found to be significantly positively related to the MMSE and MoCA scores ($p<0.05$). Likewise, the brain signal complexity in the ventral attention network was found to be significantly positively related to the MMSE and MoCA scores ($p<0.05$). These results demonstrated that more severely impaired patients tended to have reduced brain signal complexity in specific brain networks (Fig. 5).

Biomedical Optics EXPRESS

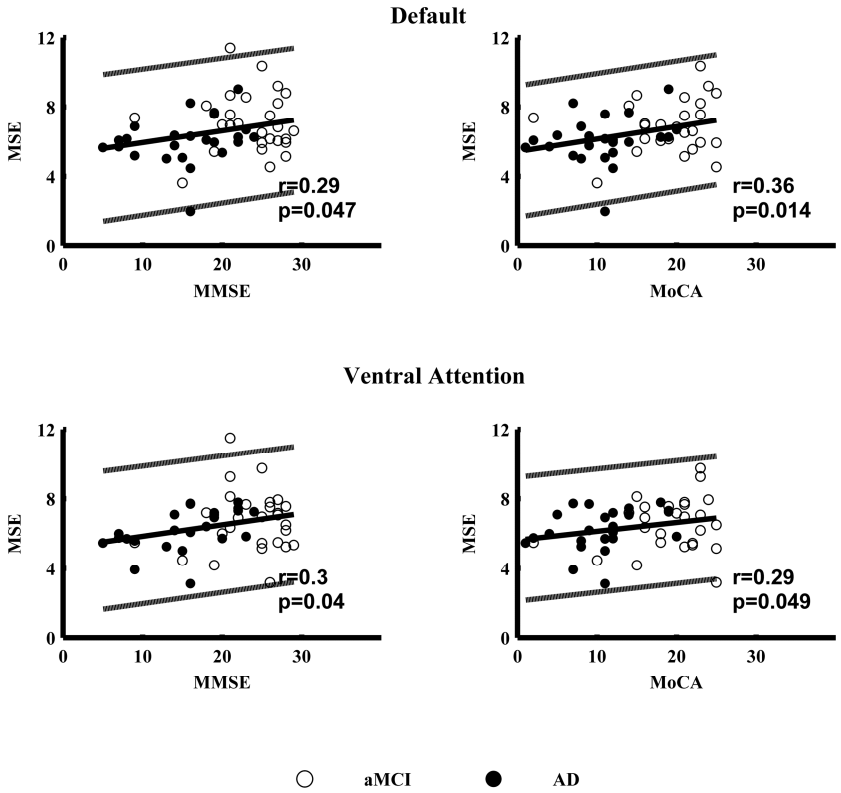

Fig. 5. Correlation analysis between brain signal complexity and clinical variables. The scatter plots between clinical variable scores and MSE values in the combined AD and aMCI groups. The dashed lines in the correlation maps are regression lines with 95% prediction error bounds.

4. Discussion

In this study, we used fNIRS to evaluate the complexity of cortical hemoglobin signals at a high temporal resolution in different brain networks of aMCI and AD patients. Our key finding is that the AD group is characterized by decreased brain signal complexity compared with the HC group. The aMCI group demonstrated intermediate signal complexity on MSE, with values falling between those of the AD and HC groups. Moreover, these reductions in signal complexity appeared to be pathophysiologically meaningful, being correlated with the scores of the MMSE and MoCA. To the best of our knowledge, the present study represents a pioneering investigation of the complexity in spontaneous hemoglobin signal activity and its relation to cognitive performance in AD patients.

The current study shows that AD patients, compared to healthy controls, exhibited a reduced resting-state fNIRS complexity in most brain regions (Fig. 3(A)) and several typical cognitive networks (Fig. 4), e.g., the default mode and ventral attention networks. This result indicated that AD patients have decreased information processing capability in the brain compared to the healthy participants. The main reasons could attribute to an extensive neuronal death, a general effect of neurotransmitter deficiency or a decrease in the brain connectivity of local neural networks [33–35]. Our findings are in accord with the hypothesis that a decrease in the complexity of spontaneous brain activity is associated with disease states and aging [9]. The sample entropy of all of the three groups in this study showed a monotonic increase from the fine scale to the coarse scale, and entropy was consistently lower in the patient groups compared with the HC group. Notably, the weakest separation among the three groups was observed for scale one, the only scale studied by traditional entropy metrics. AD patients in our study exhibit abnormally decreased hemoglobin signal complexity

Biomedical Optics EXPRESS

over higher scale factors and toward regular patterns. It is known that the brain dynamics are affected by both local dense interconnectivity and long range excitatory projections [36, 37], so neuronal activity at these two spatial scales may be modulated by different neuropathophysiological mechanisms in AD. Based on this context, complexity at different temporal scales might represent different neuropathophysiological mechanism in AD and our results of increased complexity at larger time scales could thus reflect abnormal network organization and explained in terms of a disconnection syndrome [38]. However, prior EEG studies found decreased entropy at a fine scale and increased entropy at a coarse scale in an AD group compared with an HC group, and the two types of entropy alternation were differentially associated with cognitive performance [11–14]. The exact pathophysiologic mechanisms of the two different MSE profiles remain unclear. This discrepancy may stem from the difference in signal characteristics and metrics [8]. Future studies to investigate the complexity of the cortical hemoglobin signals in AD patients, normal aging and other brain states are warranted to clarify this issue.

Specifically, for the different functional brain networks, AD patients showed significant and reliable MSE decreases in the default mode, frontoparietal, dorsal and ventral attention networks. Our results suggested large-scale neuronal network dysfunctions in AD patients from a temporal dynamic perspective of functional brain activity. The default mode network has been hypothesized to be relevant to AD, and activation alterations, amyloid-β and tau pathology have been consistently found within the default mode network as disease severity progresses [5, 39, 40]. The frontoparietal network is thought to be involved in a wide variety of tasks required to initiate and modulate cognitive control [41, 42]. Moreover, this network may play an important role in the compensatory process of MCI and AD [5]. The ventral and dorsal attention networks have been reported to show decreased functional connectivity and activation alterations during the progression of AD [5, 43, 44]. Although the physiological nature of complexity in the resting-state brain signal remains elusive, decreased complexity in these functional networks may be related to cognitive dysfunction and AD-related pathology.

In this regard, the relationship between MSE values and cognitive performance may provide some hints. Both MMSE and MoCA are the most commonly used neuropsychological tests for providing overall measures of cognitive impairment in AD patients [45, 46]. Our results showing the positive correlation between MSE values and neuropsychological test scores suggest that lower brain signal complexity is associated with a higher degree of cognitive decline. The default mode network is considered to be responsible for important cognitive functions, including monitoring the external environment, supporting internal mentation, and processing episodic memory [47, 48]. Episodic memory impairment is considered one of the core characteristics of cognitive decline in aMCI and AD. The ventral attention network is closely related to an exogenous stimuli-driven attention re-orienting process and is activated during and detection of unexpected salient targets [49]. Decreased complexity of hemoglobin signals in these two networks could be the underlying reasons behind the cognition loss in AD. These findings are consistent with the notion that the complexity of a physiologic system is often associated with its adaptive capacity [8].

There are several limitations in our study that should be noted. First, our sample size was relatively small; future analyses of a larger cohort should be carried out to validate the present results. Second, we did not identify significant differences in brain signal complexity between the aMCI and HC groups, which could have occurred because aMCI is a transitional period in the progression of AD and is considered a heterogeneous entity. However, further refinement of MSE measures and the definition of aMCI may enable new MSE-based methods to detect aMCI. Another limitation of our fNIRS-based MSE study must be noted. Low penetration depth is a known drawback of fNIRS brain imaging; thus, this methodology is limited to the investigation of complexity in hemoglobin signals from cortical regions in large-scale functional systems.

Biomedical Optics EXPRESS

5. Conclusion

The present study used the resting-state fNIRS imaging to evaluate the complexity of spontaneous brain signals in aMCI and AD patients and the relationship of complexity with cognitive performance. Our results provide a novel perspective for fNIRS imaging on study of the temporal dynamics of functional brain activity across large-scale neuronal networks. Although this study is only a first step in the analysis of MSE using fNIRS signals of AD patients, our findings highlight the potential utility of MSE-based methods as powerful, complementing approaches to understanding the pathophysiologic mechanisms of AD.

Funding

National Key Research and Development Program of China (2016YFC1306300); National Science Foundation of China (Grant No. 31371007, 81571755, 81761148026, 81430037, 81601454, 61633018, 61503326); Beijing Nature Science Foundation (7161009); Beijing Municipal government (PXM2017_026283_000002); Beijing Municipal Science & Technology Commission (Z161100002616020); Fundamental and Clinical Cooperative Research Program of Capital Medical University (16JL-L08); Health and Family Planning Commission of Shunyi District Beijing; Opening Foundation of Key Laboratory of Behavioral Science; Chinese Academy of Sciences; Natural Science Foundation of Hebei Province in China (F2016203343); China Postdoctoral Science Foundation (2015M581317).

Acknowledgment

We thank Shujie Geng for providing help in data collection.

Disclosures

The authors declare that there are no conflicts of interest related to this article.